A General Model to Predict the Iron Losses in Inverter Fed Induction Motors

A. Boglietti [1)], A. Cavagnino [1)], D.M. Ionel [3)], M. Popescu [2)], D.A. Staton[2)], S. Vaschetto[1)]

1) Politecnico di Torino – Dipartimento di Ingegneria Elettrica – ITALY
2) Motor Design Ltd. – U.K.
3) AO Smith Corp. – USA

***Abstract* –This paper presents an accurate and efficient method for predicting the iron losses in PWM inverter-fed induction motors. The method was initially proposed for the prediction of iron losses in non-oriented soft magnetic material with the same supply conditions. The proposed method requires the separation of the iron losses in the hysteresis and eddy current components and the average rectified and RMS of the PWM voltage values. Starting from the iron losses measured with sinusoidal supply and the PWM waveform characteristics, a fast and reliable prediction of the iron losses in the motor with the new voltage supply can be obtained. The proposed method has been proved on an induction motor prototype capable of providing good accuracy in iron loss measurement. The comparison between the measured and predicted iron losses with PWM supply have shown excellent agreement, confirming the validity of the method.**

Index terms: Core loss, iron losses, PWM voltage, induction motors

I. INTRODUCTION

Due to its simplicity and flexibility, the use of induction motor inverter supply is no longer subject to argument. However, several effects of the static converter on the machine are still under analysis by researchers working in the field of electrical machines and drives. In particular, one as yet unsolved problem is the accurate and easy prediction of the iron losses in inverter fed induction motors. Conversely, the techniques for the prediction of iron losses in magnetic samples such as in Epstein Frame or in toroidal samples can be considered established. In fact, in the last decade many interesting formulations for the prediction of iron losses in magnetic material have been proposed [1]-[9]. During this period the authors made their contribution with an intensive experimental campaign and proposed a formulation for the iron loss prediction passing from a sinusoidal to an arbitrary supply [11]-[22].

More recently researcher interests have been focused on the prediction of the iron losses in electrical machines with inverter supply conditions. The most popular approach is based on a Finite Element Method "FEM". In [23] and [24] excellent results have been presented by the authors. However, as well known, the FEM approach is very time consuming particularly in the preparation of models (lamination mesh, material definition, etc.) and computational time. In this work, the authors propose a fast and reliable method, based on the theoretical approach presented in [22]. The method has been validated, from the experimental point of view, using a specially built prototype. This prototype uses a plastic rotor cage, which allows the elimination of the rotor currents minimizing the error in the measurement of motor iron loss.

II. THEORETICAL APPROACH

As mentioned, the proposed method was previously proposed and adopted for the iron loss prediction in soft magnetic material, and is presented and deeply discussed in [22]. Hereafter a short summary of the theoretical basic is reported. The method is based on the separation of the iron loss in hysteresis and eddy current contributions, while in order to simplify the approach, the excess losses have not been separated from the classical eddy current contribution [25]. As widely known, the hysteresis losses and the eddy current losses can be written as:

$$P_h = a\ f\ B_p^x \tag{1}$$

$$P_{ec} = b\ f^2\ B_p^2 \tag{2}$$

where B_p is the peak value of the flux density, f is the frequency, x is the Steinmetz coefficient. In this study, x is considered to be 2. When the iron losses and the two contributions are known in sinusoidal supply, a variation of these values has to be expected depending on voltage waveform source. Making reference to an ideal inductor without winding losses, the supply voltage can be written as:

$$v(t) = N S \frac{dB}{dt} \tag{3}$$

where N is the turn number and S is the section of the magnetic core. If the supply voltage v(t) is alternate and the instantaneous value has the same sign of its first harmonic, the relation between the peak to peak value of the flux density B_{pp} and the supply voltage can be written as:

$$\int_0^T |v(t)|\ dt = 2\,N\,S\,B_{pp} \tag{4}$$

This condition on the voltage waveform assures that no minor loops are present in the main hysteresis loop. Introducing the average rectified value of an alternate voltage V_{av}, the peak value of the flux density can be written as:

$$B_p = \frac{V_{av}}{4\,N\,S} T = k \frac{V_{av}}{f} \tag{5}$$

Hysteresis and eddy current contribution under distorted voltage supply condition is analyzed using a special method, i.e. decomposing the supply voltage in harmonic series the flux density:

$$B(t)=\frac{1}{2\pi NS}\sum_{n}\frac{V_{n,max}}{n f}\sin(2\pi n f t+\varphi_n) \quad (6)$$

and the peak value of the generic harmonic $B_{n,max}$ is equal to:

$$B_{n,max}=\frac{V_{n,max}}{n}\frac{1}{2\pi f NS} \quad (7)$$

where $V_{n,max}$ is the peak value of the n^{th} harmonic. Starting from (2) and (7), the eddy currents contribution due to all flux density harmonics can be written as:

$$P_{ec}=\sigma\sum V_{n,max}^2=2\,\sigma V_{rms}^2 \quad (8)$$

with V_{RMS} the voltage RMS value and σ a constant material coefficient. Expression (8) shows that the eddy current losses depend on the RMS value of the supply voltage. Taking into account (1) and (5), the hysteresis contribution can be written as

$$P_h=\zeta\ V_{av}^x\ f^{1-x}=\zeta\ \frac{V_{av}^2}{f} \quad (9)$$

with ζ a constant material coefficient. As a consequence (9) shows that the hysteresis losses are dependent on the rectified average value of the supply voltage. It is important to underline that (9) can be used only if the supply voltage does not produce minor loops in the hysteresis cycle. Taking into account the previous results it is possible to correlate the iron losses measured in sinusoidal supply and the iron losses with an arbitrary supply voltage, when the characteristics of the voltage distortion are known. In particular, if the supply voltage is alternate and it can be represented by two half waves having constant sign in the half period, then (10) can be adopted for the iron losses prediction, where α, β are constant coefficients:

$$P_{ir}=\alpha\ V_{av}^2+\beta\ V_{rms}^2 \quad (10)$$

It is important to note, that the condition imposed on the voltage waveform is always true for the three phase PWM voltage usually adopted in low voltage industrial inverters. As a direct consequence of the imposed conditions on the supply voltage, an arbitrary alternate supply voltage can be characterized by means of the following two parameters:

$$\eta=\frac{V_{av}}{V_{av,fund}}$$
$$\chi=\frac{V_{rms}}{V_{rms,fund}} \quad (11)$$

Using these coefficients, the iron losses with an arbitrary waveform can be rewritten as reported in (12).

$$P_{ir}=\eta^2\ P_{h,sin}+\chi^2\ P_{ec,sin} \quad (12)$$

with the following meaning of the used symbols:

$P_{h,sin}$ is the hysteresis losses with sinusoidal supply,

$P_{ec,sin}$ is the eddy current losses with sinusoidal supply,

V_{av} is the voltage mean rectified value,

V_{RMS} is the voltage RMS value,

$V_{av,\,fund}$ is the fundamental voltage mean rectified value,

$V_{RMS,\,fund}$ is the fundamental voltage RMS value.

Consequently, when the separation between hysteresis and eddy current losses and the supply voltage characteristics are known the iron losses with arbitrary voltage waveform can be predicted.

III. Test Bench for Induction Motor Iron Loss Measurement

The validity of the proposed procedure for the induction motor iron loss prediction with inverter supply is the main target. As a consequence, the comparison between predicted and measured iron losses must be made using measured iron loss values with the highest possible accuracy. The iron losses are determined by the classical no-load test as imposed by the international standards such as the IEEE 112 method B. In the no-load test the following power balance is used.

$$P_{no-load}=P_{ir}+3R_s I_0^2+P_{mech0} \quad (13)$$

where $P_{no\text{-}load}$ is the absorbed electrical power, P_{ir} are the iron losses, R_s is the stator resistance, I_0 is the no-load current and P_{mech0} are the mechanical losses in no-load condition.

It is important to highlight that the iron losses computed by (13) must be considered as conventional ones. In fact, taking into account all the actual losses inside the machine a more accurate no-load power balance can be defined by (14)

$$P_{no-load}=P_{ir}+3R_s I_0^2+P_{mech0}+P_{ad-0} \quad (14)$$

where $P_{add\text{-}0}$ are the additional losses in no-load condition. The loss contribution due to the mechanical losses in no-load condition can be nullified performing a no-load test at synchronous speed connecting the motor under test to a synchronous motor with the same pole pair.

Among the several contributions to the additional losses in no-load conditions, the rotor cage joule losses due to the harmonic currents induced by the winding spatial harmonics have a considerable contribution. Unfortunately, these losses cannot be segregated from the conventional iron losses and when (13) is used, these additional rotor losses are erroneously attributed to the iron losses.

As a consequence, the conventional iron losses are not the most accurate quantity to be considered for a good comparison with computed ones. In order to overcome this limitation a special rotor with a rubber cage has been cast.

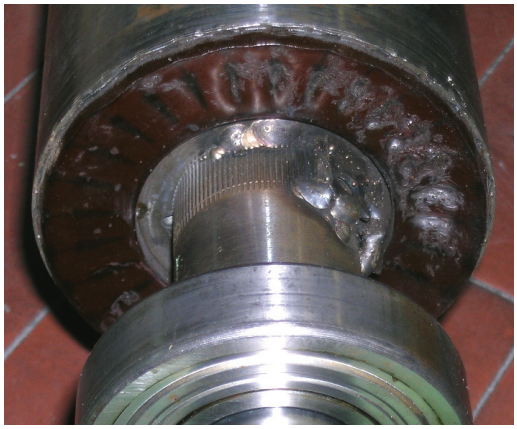

Fig.1: Plastic rotor cage used for the iron losses measurement.

The rotor cage used is shown in Fig. 1. As discussed in [26], no load tests at synchronous speed have shown that the additional losses due to the rotor harmonic currents are not negligible with respect to actual iron losses. As a consequence, in order to obtain more accurate values for the iron losses, all the experimental tests used for the validation of the proposed method have been performed using this rubber rotor prototype.

The prototype has been assembled using a lamination material previously tested on an Epstein frame for obtaining the loss contribution separation, following the procedure described in [22]. As a consequence, all the elements requested for the iron losses prediction with arbitrary voltage supply are available. As the rotor is not able to run by itself due to the plastic rotor cage, the rotor prototype is driven using a synchronous machine with same pole pair. In order to avoid the presence of slip (and related rotor iron losses) during the no load at synchronous speed, the supply frequency must be the same both for the motor under test and the synchronous motor. This condition was easily obtained for the tests with sinusoidal supply; however, for the inverter supply this condition could not be replicated due to the impossibility of synchronizing the fundamental frequency of the inverter with the sinusoidal power supply of the synchronous motor. After some no-load tests at synchronous speed with inverter supply, it was evidently impossible to achieve the condition of zero slip. In particular, the test results were not constant with a large spread of the prototype absorbed electrical power with the same electrical condition. As any torque and speed transducer was connected between the two machine shafts, the mechanical power, exchanged between the two machines, was not measurable. Using (14) to determine the iron losses contribution, this exchanged power could wrongly be attributed to the motor under test iron losses, with significant reduction of the method accuracy. Nonetheless, it is important to underline that the main target of this work is to evaluate the accuracy of the proposed method and as a consequence, an alternative solution to the no-load test at synchronous speed has been found. In fact, in the absence of a conductive rotor cage, when the rotor is still the rotor cage copper losses are zero and the prototype is in the same magnetic condition of the no-load test at synchronous speed. For the considered prototype, the difference between the locked rotor test and the synchronous no-load test is due to the presence of the iron losses in the rotor at the same frequency of the stator. In other word, if the tests with sinusoidal and PWM supply are performed with the rotor in stand-still condition, all the stator and rotor iron losses are measured and the proposed method can be applied considering all the iron losses active in the machine. This approach allows the use of (14) with excellent accuracy.

IV. Measured and Computed Results: Comparison and Discussion

During the tests with PWM supply, for each measured point the coefficient values η and χ values have been computed and used for predicting the iron losses starting from the same value with sinusoidal supply. As previously discussed, the proposed method is based on the separation of the iron losses in the hysteresis and in the eddy current components. The percentage of the two loss components is dependent on the flux density [14], [17]. At constant voltage, in magnetic sample, the flux density is considered constant in all the material, while in electrical machines the flux density changes in the lamination. As a consequence the ratio between hysteresis and eddy current losses is variable in the different points of the machine lamination.

To account for loss coefficient variations with flux-density and frequency, the authors are using the model that extends previous research results [17-22] and allows the hysteresis loss coefficient to vary with frequency and flux-density. Meanwhile, the classical loss and anomalous loss are grouped into an eddy-current loss term, where the corresponding coefficient varies with flux-density and frequency level:

$$\begin{aligned} P_{\mathrm{h,sin}} &= k_{\mathrm{h}}\left(f,B\right)\cdot f\,B^2 \\ P_{\mathrm{ec,sin}} &= k_{\mathrm{e}}\left(f,B\right)\cdot\left(f\,B\right)^2 \end{aligned} \tag{15}$$

Several functions have been tried to describe the k_{e} loss coefficients variation with the induction level. The lowest relative error values and the simplicity of implementation are provided by third order polynomials:

$$k_{\mathrm{e}}(B) = k_{\mathrm{e3}}B^3 + k_{\mathrm{e2}}B^2 + k_{\mathrm{e1}}B + k_{\mathrm{e0}} \tag{16}$$

Depending on the frequency range of the iron loss data considered, different curves for k_{e} and k_{h} as a function of the induction are obtained. Previously obtained results [14], [17], [22] demonstrate that the eddy-current loss coefficient k_{e} increases with the induction level and decreases with the frequency. A third order polynomial is employed for the coefficient k_{h} that will have an induction variation of the form:

$$k_{\mathrm{h}}(B) = k_{\mathrm{h3}}B^3 + k_{\mathrm{h2}}B^2 + k_{\mathrm{h1}}B + k_{\mathrm{h0}} \tag{17}$$

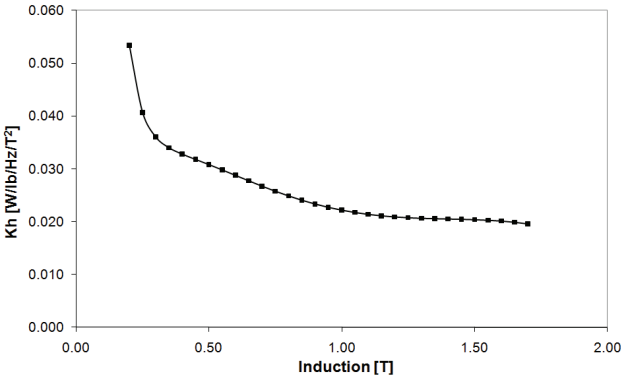

Fig. 2: Hysteresis loss coefficient k_h variation with flux-density for frequency up to 200Hz

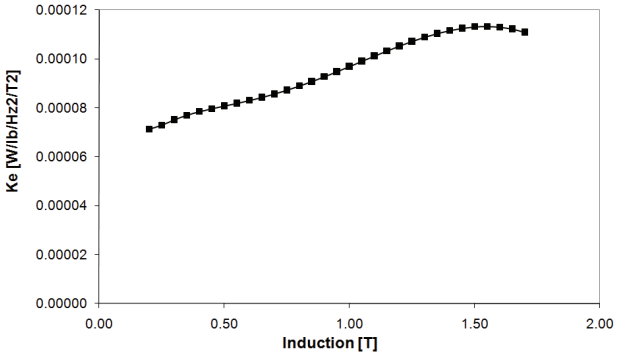

Fig. 3: Eddy-current loss coefficient k_e variation with induction for frequency up to 200Hz

In the employed model, within a given frequency range, k_e and k_h are dependent only on B, which provides a more straight forward computation of the hysteresis and eddy-current loss components. Depending on the set frequency range, the polynomial functions that describe the loss coefficients k_e and k_h will have different variations. It is important to note that the higher relative error for the estimated losses at lower induction levels may be significantly reduced if a higher polynomial function, i.e. 4^{th} order is used for the estimation of the hysteresis loss coefficient k_h.

Figs. 2 and 3 show the variation of the loss coefficients with flux-density when the fundamental frequency range is up to 200Hz. These values are applied for the tested induction motor, as the fundamental supply frequency is 50Hz.

The authors have successfully fitted the model described by (10-12) and (15) to laminated steels typically employed in electric motor manufacturing, such as semi-processed and fully-processed materials under PWM voltage supply [22].

For the estimation of the iron losses in the induction motor a combination of analytical formulations and finite-element analysis is employed.

Fig. 4 shows the cross-section of the test induction motor, a 4-pole, 36-slots, 28-bars configuration. The rotor bars are of Boucherot type to ensure high starting torque and high efficiency at rated load. The motor data is given in Annex I.

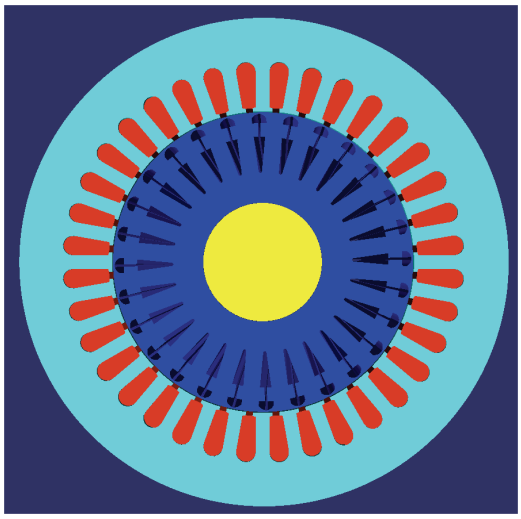

Fig. 4: Cross section of the analysed induction motor

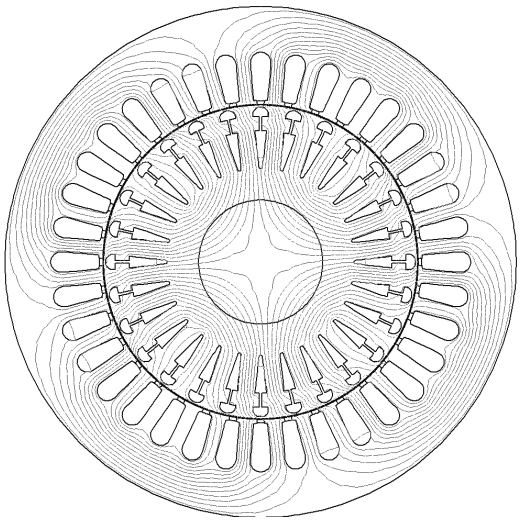

Fig. 5: Finite-element flux-plot of the analyzed induction motor

Fig. 5 shows the simulated flux-lines plot for one of the performed experimental test. Unlike in the Epstein test, the typical flux density waveform in electrical machines is non-sinusoidal [17-20]. To account for this, some other authors have extended similar expression for (1) and (2) into the time domain by replacing the frequency with a time derivative [27]. Although not always clearly stated, such an approach is strictly valid only provided that the material coefficients are constant. Also, the slotting effect is the main cause of the minor hysteresis loops and the flux-density waveform especially in the tooth tips may contain reversals, causing minor loops and increased hysteresis loss.

In the proposed model (12)-(17), the material coefficients are frequency and flux density dependent, therefore a time-dependent or a harmonic model may be employed. As the magnetic properties of the steel are non-linear the use of a harmonic model is itself debatable, and this engineering

approach should be carefully used especially if the contribution of a high order harmonic is expected to be comparable with that of the fundamental wave.
If the magnetization B waveform is decomposed in a Fourier series of harmonics, equation (15) may be substituted with the sum of the contribution of the harmonics. Each harmonic effect may be easily identified for both terms in (2) within a given range. The hysteresis loss and the eddy current loss components are:

$$P_{\text{iron}} = \sum_{n=1}^{N} P_{\text{h}n} + \sum_{n=1}^{N} P_{\text{ec}n} \tag{18}$$

where:

$$P_{\text{ec,n}} = k_{\text{e}}(B_n) f^2 n^2 B_n^2 \tag{19}$$

$$P_{\text{h,n}} = k_{\text{h}}(B_n) f n B_n^2 \tag{20}$$

The computation algorithm of the iron losses is described as follows:

1. A transient magnetic voltage driven 2D finite-element problem is defined. The supply voltage is modelled as sinusoidal 3-phase system, the rotor is kept fixed and the rotor cage is modelled as an open circuit using very high resistivity for the rotor bars and end-rings. In this way, the rotor cage is not shielding the rotor steel any more, as well evident in Fig.5. This analysis was performed using Flux2D software, but the same approach should be taken in any other similar FE package.
2. From the magnetic field solution is extracted the flux-density waveform corresponding to an electric cycle for each mesh element from the iron regions, i.e. stator and rotor steel. Note that the shaft region is neglected in this study. The flux-density is analysed per components, radial and tangential. In the induction motor prototype a significant amount of iron losses are produced in the stator yoke, where the flux density has both a radial and a tangential component (Fig. 6). In the stator teeth the flux-density has essentially just the radial component (Fig. 7). The stator tooth tips represent a special region where both radial and tangential flux-density components have relevant values (Fig. 8).
   Particularly at and above rated voltage, this problem is very challenging because of the extremely high value of the flux density.
3. Fourier series decomposition is applied for all the flux-density waveforms The first 11$^{\text{th}}$ harmonic orders are considered for practical reasons.
4. Equations (18-20) are applied to compute the iron losses in each mesh element of the iron regions.
5. Summation of all the losses per element gives the total iron loss under sinusoidal voltage supply (15). Fig. 9 shows the iron loss distribution under sinusoidal supply voltage conditions. The highest iron loss density is predicted in the stator teeth region.
6. Apply relation (12) to account for PWM voltage supply.

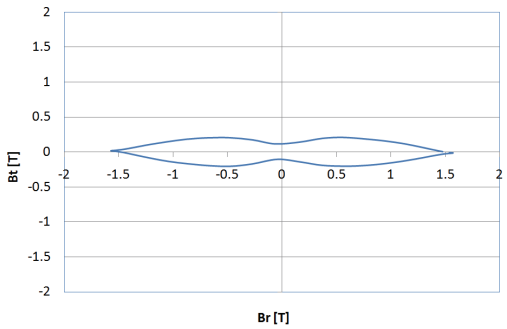

Fig. 6: Radial and tangential components of the flux-density measured in the middle of the stator yoke.

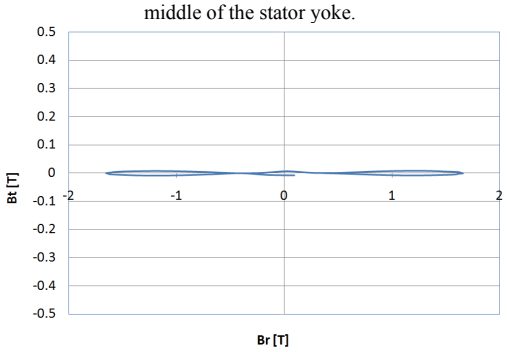

Fig. 7: Radial and tangential components of the flux-density in the middle of the stator tooth.

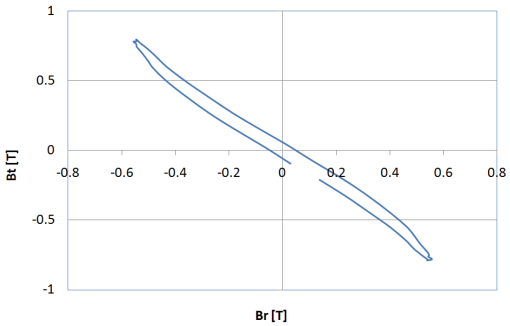

Fig. 8: Radial and tangential components of the flux-density in the stator tooth tip.

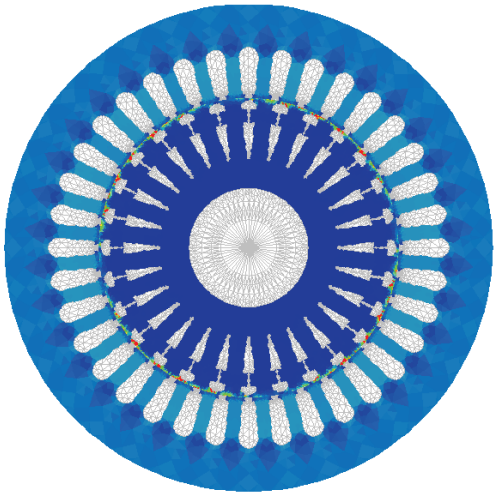
Fig. 9: Iron loss density in the induction motor prototype.

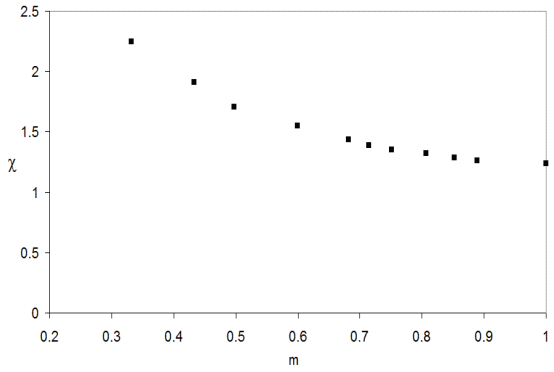

Fig. 10: Variation of parameter χ with inverter PWM modulation index *m*.

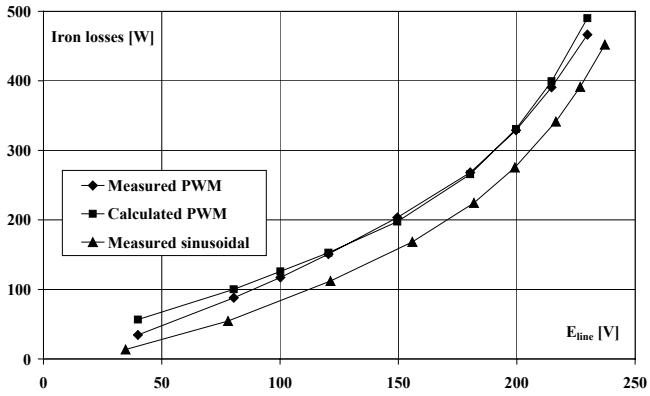

Fig.11: Predicted and measured iron losses with PWM supply (fundamental frequency = 50 Hz, switching frequency = 2 kHz, variable modulation index)

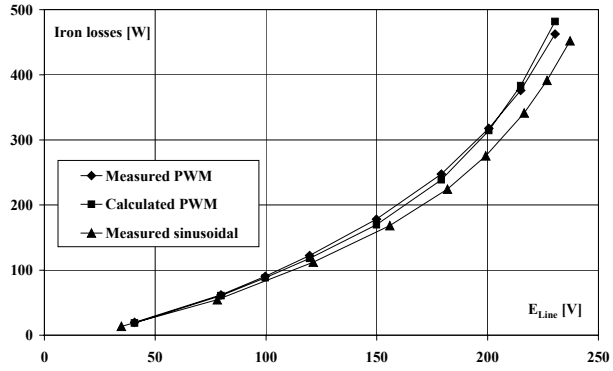

Fig. 12: Predicted and measured iron losses with PWM supply (fundamental frequency = 50 Hz, switching frequency = 2 kHz, variable DC bus voltage).

The tests with PWM supply have been performed for a fundamental 50 Hz and a switching frequency of 2 kHz. The tests have been performed with variable modulation index (fixed DC bus voltage) and with variable DC bus voltage (fixed modulation index). In all the tests a sinusoidal modulation waveform was adopted. If the ratio between the carrier frequency and the modulation frequency is high, the η coefficient (11) is typically equal to unity, as verified in a high number of measurements on the three phase PWM inverter.

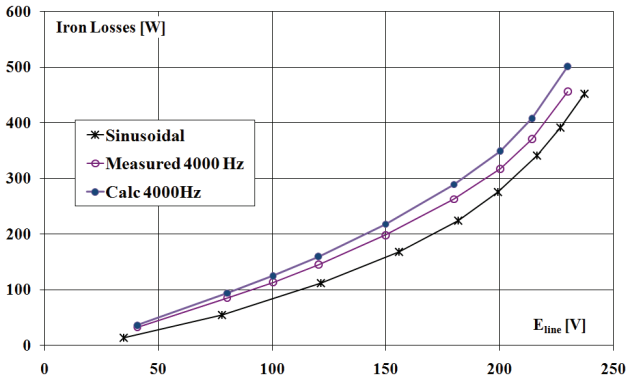

Fig.13: Predicted and measured iron losses with PWM supply (fundamental frequency = 50 Hz, switching frequency = 4 kHz, variable modulation index)

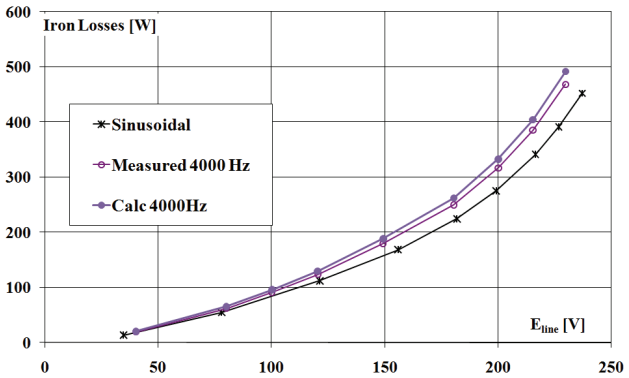

Fig. 14: Predicted and measured iron losses with PWM supply (fundamental frequency = 50 Hz, switching frequency = 4 kHz, variable DC bus voltage).

As a consequence, in this case, the increase in iron loss with a PWM supply is solely due to an increase in dynamic hysteresis (eddy-currents) loss. In an initial set of experiments the inverter PWM modulation index *m* was maintained constant to a value of 1. The computed value of the parameters χ and η varied around the values of 1.20 and 1 respectively. In this case, the estimated iron losses under PWM supply are actually scaled from those obtained with sinusoidal supply, by using constant factors for the modelling of the increase in the dynamic (eddy-currents) and static (hysteresis) iron loss components.

A second round of experiments was performed with a variable modulation index in between 0.3 and 1. The parameter χ, which accounts for the dynamic iron loss increase under PWM supply, varied as shown in Fig. 10. As expected, the parameter η, which models the static iron loss increase, was practically unchanged and a constant value of 1 was used in the calculations.

Fig. 11, 13, 15 show the comparison between the measured and predicted iron losses for a variable modulation index and switching frequency of 2kHz, 4kHz and 6kHz respectively. Figs. 12, 14, 16 show the comparison between the measured and predicted iron losses for a variable DC bus voltage and switching frequency of 2kHz, 4kHz and 6kHz respectively.

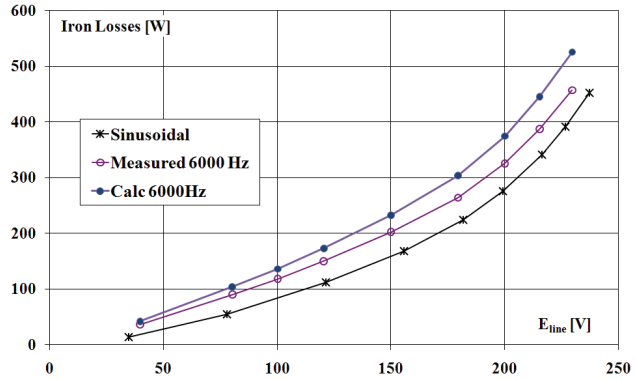

Fig.15: Predicted and measured iron losses with PWM supply (fundamental frequency = 50 Hz, switching frequency = 6 kHz, variable modulation index)

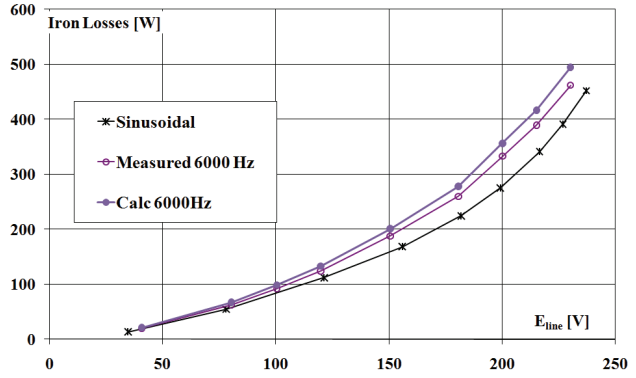

Fig. 16: Predicted and measured iron losses with PWM supply (fundamental frequency = 50 Hz, switching frequency = 6 kHz, variable DC bus voltage).

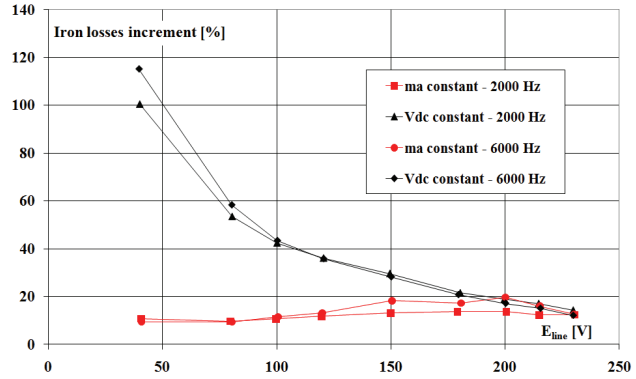

Fig. 17: Measured iron loss increment for switching frequencies of 2kHz and 6kHz.

In all cases an excellent agreement between the measured and the predicted values is observed. The relative errors are in the range of 5% to 15%, where relative error is defined as the ratio between the differences in the calculated versus test data and the test data.

Two important aspects have to be noted regarding the level of iron losses in induction motors under PWM supply:

- Losses are mainly determined by the fundamental frequency i.e. 50Hz for the test motor. The switching frequency plays a minor role in the iron loss mechanism.
- Losses are higher when a control strategy with variable modulation index and constant voltage DC bus is employed. For the test motor an increase of approximately 20% is observed (Fig. 17).

The proposed method can be successful used not only for the estimation of the losses in laminated steel sheets, but also for the iron loss prediction in induction motors. Further studies are currently underway for the estimation of iron losses in brushless PM AC motors fed from PWM current inverters.

V. Conclusions

In this paper a method proposed by the authors for the prediction of iron losses with PWM supply in magnetic material has been applied for induction motors analysis. In order to eliminate certain uncertainties in the iron loss measurement a special prototype with plastic rotor cage has been built. The results have proven the methods validity, with very good agreement between the measured and the predicted iron losses in the induction motor with PWM supply.

Annex I

MOTOR PARAMETERS

3-PHASE INDUCTION MOTOR: 4-POLE, 230 V, 11KW

Parameter	*Value*
Connection	Delta
Slots	36
Bars	28
Skew angle	0
Stator phase resistance @20C [ohms]	0.305
Rotor resistance @ 20C [ohms]	0.314
Stator leakage inductance @ locked rotor condition [mH]	4.3
Rotor leakage inductance @ locked rotor condition [mH]	5.0
Magnetizing reactance @ no-load conditions [mH]	110
Rated torque [Nm]	79
Rated phase current [ARMS]	22.5
Rated speed [rpm]	1440
Efficiency [%]	89.2

References

[1] F. Fiorillo, A. Novikov, “Power losses under sinusoidal, trapezoidal and distorted induction waveform”, IEEE *Transactions on Magnetics*, Vol. 26, September 1990, pp. 2559-2561.

[2] R. Kaczmarek, M. Amar, “A general formula for prediction of iron losses under non-sinusoidal supply voltage waveform ”, *IEEE Transactions on Magnetics*, Vol. 31, No. 5, September 1995, pp. 2505-2509.

[3] R. Kaczmarek, M. Amar, F. Protat, “Prediction of power losses in silicon iron sheets under PWM voltage supply”, *Journal of Magnetism and Magnetic Materials*, No. 133, 1995, pp. 140-143.

[4] R. Kaczmarek, M. Amar, F. Protat, “Iron losses under PWM voltage supply on Epstein frame and in induction motor core”, *IEEE Transactions on Magnetics*, Vol. 32, No. 1, January 1996, pp. 189-194.

[5] C. Cester, A. Kedous-Lebouc, B. Cornut, “Iron loss under practical working conditions of a PWM powered induction motor”, *IEEE Transactions on Magnetics*, Vol. 33, September 1997, pp. 3766-3768.

[6] E. Barbisio, F. Fiorillo, C. Ragusa, “Predicting loss in magnetic steels under arbitrary induction waveform and with minor hysteresis loops”, *IEEE Transactions on Magnetics*, , Vol. 40, No. 4, Part 1, July 2004, pp. 1810-1819.

[7] T.L. Mthombeni, P. Pillay, “Core losses in motor laminations exposed to high-frequency or non-sinusoidal excitation”, *IEEE Transactions on Industry Applications*, Vol. 40, No. 5, September-October 2004, pp. 1325-1332.

[8] Z. Gmyrek, J. Anuszczyk, “The power loss calculation in the laminated core under distorted flux conditions”, Conf. rec. International Conference on Electrical Machines, ICEM2004, Krakow, Poland, on Cd-Rom.

[9] P.J Leonard, P. Marketos, A.J. Moses, M. Lu, “Iron losses under PWM excitation using a dynamic hysteresis model and finite elements”, *IEEE Transactions on Magnetics*, Vol. 42, No. 4, April 2006, pp. 907-910.

[10] Boglietti, P. Ferraris, M. Lazzari, M. Pastorelli, “Change of the iron losses with the switching supply frequency in soft magnetic materials supplied by PWM inverter”, *IEEE Transactions on Magnetics*, Vol. 31, No. 6, November 1995.

[11] Boglietti, P. Ferraris, M. Lazzari, M. Pastorelli, “Influence of modulation techniques on iron losses with single phase DC/AC converter”, *IEEE Transactions on Magnetics*, Vol. 32, No. 5, September 1996.

[12] Boglietti, M. Lazzari, M. Pastorelli, “Iron losses prediction with PWM inverter supply using steel producer datasheets”, Conf. Rec. IEEE-IAS'97 Annual Meeting, 5-9 October, New Orleans 1997, USA.

[13] Boglietti, A. Cavagnino, M. Lazzari, M. Pastorelli, “Two simplified methods for the iron losses prediction in soft magnetic materials supplied by PWM inverter”, Conf. Rec. IEEE International Electric Machines and Drives Conference 2001, IEMDC’01, 17-20 June 2001, Boston, USA.

[14] A.Boglietti, A. Cavagnino, M. Lazzari, M. Pastorelli, “Predicting iron losses in soft magnetic materials with arbitrary voltage supply: an engineering approach”, *IEEE Transactions on Magnetics*, Vol. 39, March 2003, pp. 981-989.

[15] Boglietti, A. Cavagnino, Z. Gmyrek, “Iron Losses Prediction with PWM Supply Using Low and High Frequency Measurements: Analysis and Results Comparison”, *IEEE Transaction on Industrial Electronics*, Vol.55, No. 4, April 2008, pp.1722-1728.

[16] D.M Ionel, M. Popescu, S.J. Dellinger, T.J.E Miller, R.J Heideman, M.I McGilp, “Factors Affecting the Accurate Prediction of Iron Losses in Electrical Machines”, Electric Machines and Drives, 2005 IEEE International Conference on 15-15 May 2005 Page(s):1625 – 1632.

[17] D.M. Ionel, M. Popescu, S.J Dellinger, T.J. Miller, R.J. Heideman, M.I McGilp, “On the variation with flux and frequency of the core loss coefficients in electrical machines”, *IEEE Transactions on Industry Applications*, Vol. 42, No. 3, May-June 2006, pp. 658-667.

[18] M. Popescu; D.M. Ionel, “A Best-Fit Model of Power Losses in Cold Rolled Motor Lamination Steel Operating in a Wide Range of Frequency and Magnetization” *IEEETrans. on Magnetics, Vol. 43, No. 4, Apr. 2007, pp. 1753-175*6.

[19] M.Popescu, T.J. Miller, D.M.Ionel, S.J. Dellinger, R. Heidemann, “On the Physical Basis of Power Losses in Laminated Steel and Minimum-Effort Modeling in an Industrial Design Environment” 42nd I*AS Annual Meeting, 23-27* Sept. 2007, pp. 60 – 66.

[20] M.Popescu; D.G.Dorrell, D.M.Ionel, “A Study of the Engineering Calculations for Iron Losses in 3-phase AC Motor Models”, 33rd IECON 2007, 5-8 Nov. 2007, pp. 169 – 174.

[21] D.M.Ionel, M.Popescu, M.McGilp, T.J. Miller, S.Dellinger, R.J. Heideman, “Computation of Core Losses in Electrical Machines Using Improved Models for Laminated Steel”, *IEEE Trans. on Industry Applications*, Vol. 43, No. 6, Nov./Dec 2007,pp. 1554-1564.

[22] D.M. Ionel, M. Popescu, C.Cossar, M. I. McGilp, A.Boglietti, A.Cavagnino, “A Gener*al Model of the Laminated Steel Loss*es in Electric Motors with PWM Vol*tage Supply”, Industry Applications* Society Annual Meeting, 2008. IAS '08. IEEE, 5-9 Oct. 2008 pp. 1-7.

[23] A. Boglietti, A. Cavagnino, Z. Gmyrek, “Estimation and analysis of iron losses in induction motor under sinusoidal and PWM excitation”, Conf. Rec. International Conference on Electrical Machines, ICEM 2008, Vilamoura, Portugal, on CD-Rom.

[24] Boglietti, A. Cavagnino, A.M. Knight, “Isolating the impact of PWM modulation on iron losses”, Con. Rec. IEEE-IAS’08 Annual Meeting, 2008, Edmonton, Canada, on Cd-Rom.

[25] G. Bertotti, “Physical interpretation of eddy current losses in ferromagnetic materials. I. Theoretical considerations”, *Journal of Applied Physic*, No. 57, March 1985, pp. 2110-2117.

[26] Boglietti, A. Cavagnino, M. Lazzari, M. Pastorelli, “A Critical Approach to the Iron Losses in Induction Motors”, Energy Efficiency in Motor Driven System pp, Springer-Verlag, ISBN 3-540-00666, pp. 71-77.

[27] M. A. Mueller, S. Williamson, T. Flack, K. Atallah, B. Baholo, D. Howe, and P. Mellor, “Calculation of iron losses from time-stepped finite-element models of cage induction machines,” in *Conf. Rec. IEE EMD’95,* Durham, UK, Sept. 1995, pp. 88–92.

[28] H. Domeki, Y. Ishihara, C. Kaido, Y. Kawase, S. Kitamura, T. Shimomura, N. Takahashi, T. Yamada, and K. Yamazaki, “Investigation of benchmark model for estimating iron loss in rotating machine,” *IEEE Trans. on MAG*, vol. 40, no. 2, pp. 794–797, Mar. 2004.

[29] Y. Chen and P. Pillay, “An improved formula for lamination core loss calculations in machines operating with high frequency and high flux density excitation,” in *IEEE 37th IAS Annual Meeting Conf. Rec.*, Pittsburgh, PA, Oct. 2002, pp. 759–766.